Available online at www.sciencedirect.com

SciVerse ScienceDirect

Geochimica et Cosmochimica Acta 93 (2012) 63–76

Geochimica et Cosmochimica Acta

www.elsevier.com/locate/gca

Platinum group element abundances in the upper continental crust revisited – New constraints from analyses of Chinese loess

Jung-Woo Park [a], Zhaochu Hu [b,c,*], Shan Gao [b,c], Ian H. Campbell [a], Hujun Gong [c]

[a] Research School of Earth Sciences, Australian National University, Canberra 0200, ACT, Australia
[b] State Key Laboratory of Geological Processes and Mineral Resources, Faculty of Earth Sciences, China University of Geosciences, Wuhan 430074, PR China
[c] State Key Laboratory of Continental Dynamics, Department of Geology, Northwest University, Xi'an 710069, PR China

Received 2 December 2011; accepted in revised form 23 June 2012

Abstract

Platinum group element (PGE) abundances in the upper continental crust (UCC) are poorly constrained with published values varying by up to an order of magnitude. We evaluated the validity of using loess to estimate PGE abundances in the UCC by measuring these elements in seven Chinese loess samples using a precise method that combines NiS fire assay with isotope dilution. Major and trace elements of the Chinese loess show a typical upper crustal composition and PGE abundances are consistent with literature data on Chinese loess, except for Ru, which is a factor of 10 lower than published values. We suggest that the high Ru data and Ru_N/Ir_N values of Chinese loess reported by Peucker-Ehrenbrink and Jahn (2001) (*Geochem. Geophys. Geosys.* **2**, 2001GC000172) are an analytical artifact, rather than a true geochemical characteristic of loess because likely sources of loess are not significantly enriched in Ru and transport and deposition processes cannot preferentially enrich Ru in loess. The effect of eolian fractionation on PGE abundances in loess appears to be limited because Chinese loess from different locations shows similar PGE patterns and concentrations. This conclusion is supported by strong positive correlations between the PGE (except for Pt) and other compatible elements such as Fe_2O_3, Ni, Cr, Co. Using a compilation of PGE data for loess from China, Argentina and Europe, including our data but excluding one sample with an anomalously high Pt content, we propose average PGE abundances for global loess of Ir = 0.022 ppb (ng/g), Ru = 0.030 ppb, Rh = 0.018 ppb, Pt = 0.599 ppb, and Pd = 0.526 ppb, and suggest that these are the best current estimates for the PGE abundances of the UCC.

1. INTRODUCTION

The Platinum group elements (PGEs) comprise a select group of transition metals that show a strongly siderophile (iron-loving) character, and are therefore overwhelmingly concentrated in the Earth's core. As a result, PGE levels in the complementary silicate portion of the Earth are vanishingly low, particularly in the highly evolved upper continental crust, samples of which therefore present a significant analytical challenge. Due to their low abundances in the continental crust, the PGE concentrations in impact melts and sediments related with impact events have been used as sensitive indicators of extraterrestrial influx (e.g. Schmidt and Pernicka, 1994; Schmidt et al., 1997; Tagle et al., 2004; Tagle and Berlin, 2008; Paquay et al., 2009). In addition, as the consumption of Rh, Pt and Pd in the auto-catalysts industry increases, knowledge of PGE concentrations and distribution characteristics in urban environments becomes paramount. In such studies, the PGE abundances of the upper continental crust (UCC) are used as a natural background for urban roadside soil samples (e.g. Fritsche and Meisel, 2004; Hooda et al., 2008; Pan et al., 2009; Wang and Sun, 2009).

* Corresponding author at: State Key Laboratory of Geological Processes and Mineral Resources, Faculty of Earth Sciences, China University of Geosciences, Wuhan 430074, PR China.
E-mail address: zchu@vip.sina.com (Z. Hu).

0016-7037/$ - see front matter © 2012 Elsevier Ltd. All rights reserved.
http://dx.doi.org/10.1016/j.gca.2012.06.026

Despite its significance, the average PGE composition of the UCC is poorly constrained with published values varying by up to an order of magnitude. The variation results from a diverse range of methods and sample types being applied to the problem. There have been four different approaches: (1) Schmidt et al. (1997) proposed PGE concentrations in impact melts as regional averages of the UCC in target areas after eliminating their meteoritic contributions, (2) Taylor and McLennan (1985) and Gao et al. (1998) reported estimates for average upper crustal PGE concentrations based on a large number of individual rock analyses representative of the UCC, (3) Wedepohl (1995) reported average PGE concentrations in 17 graywackes from Europe, (4) Peucker-Ehrenbrink and Jahn (2001) proposed that the average PGE concentrations of 16 loess samples from China, Argentina and Europe could be taken as an estimates for the UCC. In their study, the average Ru concentration of Chinese loess is a factor of 5 higher than that of European loess, although the concentrations of the other PGE are similar to each other. This discrepancy requires an explanation.

Loess consists of wind-blown sediments, and is formed under arid glacial conditions. Importantly, the grains are derived from wind erosion of crustal rocks covering large geographical areas without having undergone extensive chemical weathering (Smalley, 1966, 1995), thereby conserving and homogenizing the composition of the UCC. As such, the composition of loess has been used as an estimate for the UCC (e.g. Taylor et al., 1983; Gallet et al., 1998; Barth et al., 2000; Peucker-Ehrenbrink and Jahn, 2001; Hu and Gao, 2008). In this study we analyzed seven samples of Chinese loess for Ir, Ru, Rh, Pt, Pd, and Re abundances using a combined Ni–sulfide fire assay – isotope dilution (NiS-FA-ID) method and an Agilent 7700x ICP-MS. The Agilent 7700x ICP-MS has the lowest argide production levels among conventionally used quadrupole ICP-MS systems (Guillong et al., 2011), which allowed the accurate measurement results of PGE concentrations, especially Ru. We also report the first Rh concentrations in loess. Our data, together with previously reported PGE contents in loess (Peucker-Ehrenbrink and Jahn, 2001), were used to re-examine the validity of using PGE concentrations in loess for estimating the average composition of the UCC.

2. SAMPLES AND ANALYTICAL METHODS

The loess samples used in this study were collected from four different sections of the Chinese Loess Plateau (Fig. 1, Table 1): Wubao (Wang, 2006; Guan et al., 2008), Lantian (Sun et al., 1997), Luochuan (An et al., 1991), Lingtai (Sun et al., 1998). These four locations, taken together with the three locations (Xifeng, Xining, Jixian) of Peucker-Ehrenbrink and Jahn (2001), cover most of the Chinese Loess Plateau (Fig. 1).

The samples were powdered in an agate mortar mill (RS200, Retsch, Germany) prior to analysis. Major element compositions were analyses by XRF (RIX2100, Japan) on fused glass disks at Northwest University in Xi'an, China. As reported in Table 2, analysis of basalt reference materials BCR-2 (USGS) and GSR-3 (Chinese National standard) indicates that both precision and accuracy are better than 5%.

Whole rock trace element compositions were determined by ICP-MS (Agilent 7700x) after high-pressure acid digestion of samples in Teflon bombs at the State Key Laboratory of Geological Processes and Mineral Resources, China University of Geosciences. Sample decomposition was carried out as follows: (1) 50 mg of sample powder was weighed and placed in a home-made PTFE-lined stainless steel bomb. (2) After wetting with a few drops of ultrapure water, 1 ml of 68% v/v HNO_3 and 1 ml of 40% v/v HF were slowly added. (3) The sealed bomb was heated at 190 °C in an electric oven for 48 h. (4) After cooling, the bomb was opened and placed on a hot-plate at 120 °C, and evaporated to incipient dryness (but not baked). (5) 1 ml HNO_3 was then added and evaporated to dryness. (6) The residue was re-dissolved by adding 1 ml of HNO_3, 1 ml of ultra-pure water and 1 ml of 1 μg/ml In internal standard solution. (7) The bomb was then resealed and placed in an electric oven at 150 °C for 12 h. (8) The final solution was transferred to a polyethylene bottle and diluted to 100 g by addition of 2% v/v HNO_3.

The instrument was optimized to obtain maximum signal intensities for Li, Y, Ce and Tl, while keeping the CeO^+/Ce^+ and Ce^{2+}/Ce^+ ratios below 1.2%. A rock solution was flushed through the instrument for 30 min prior to tuning to minimize drift. Drift corrections were carried out using In as an internal standard, which was repeatedly analyzed over the duration of a run. Table 3 shows results for four USGS reference materials (BCR-2, BHVO-2, AGV-2, SCo-1). Analytical precision reported as 1 × RSD (%) is generally better than 8% for most elements except for Cd (8.4%-14%), W (8.3%-13%) and Bi (12–18%) in BCR-2, BHVO-2 and AGV-2, and Cd (22%) and Bi (9.9%) in SCo-1, which are mainly caused by the low analyte concentrations in these samples. Our measured values for the international reference materials are compared with the values from the GeoReM database (http://georem.mpch-mainz.gwdg.de/) and Govindaraju (1994) in Table 3. The agreement between our data and the reference values is better than 8% for most of the elements in these geological reference samples.

PGE and Re concentrations were measured using a Ni–sulfide fire assay – isotope dilution method. The analytical details are presented in Park et al. (2012) and Appendix A. Briefly, a solution spiked with enriched isotopes (^{99}Ru, ^{105}Pd, ^{185}Re, ^{191}Ir, and ^{195}Pt) was added to a mixture of sample (10 g), Ni (1 g), S (0.5 g) and Na-borax (10 g). The spiked mixture was placed in a crucible, fused in a furnace under reducing conditions, and quenched by removing the crucible from the furnace. The reducing conditions were provided by using a second outside crucible that contains about 0.1 g of flour and by introducing N_2 gas into an open furnace, which helped ensure good spike-sample equilibration and recovery of Re. After quenching, the crucible was broken open and the Ni–sulfide beads were collected and dissolved in 6 mol/l HCl. The solution was then filtered through a Millipore filter paper and the paper was digested in aqua regia. After complete digestion, the solution was dried down, diluted with 2% v/v HNO_3, and refluxed. This

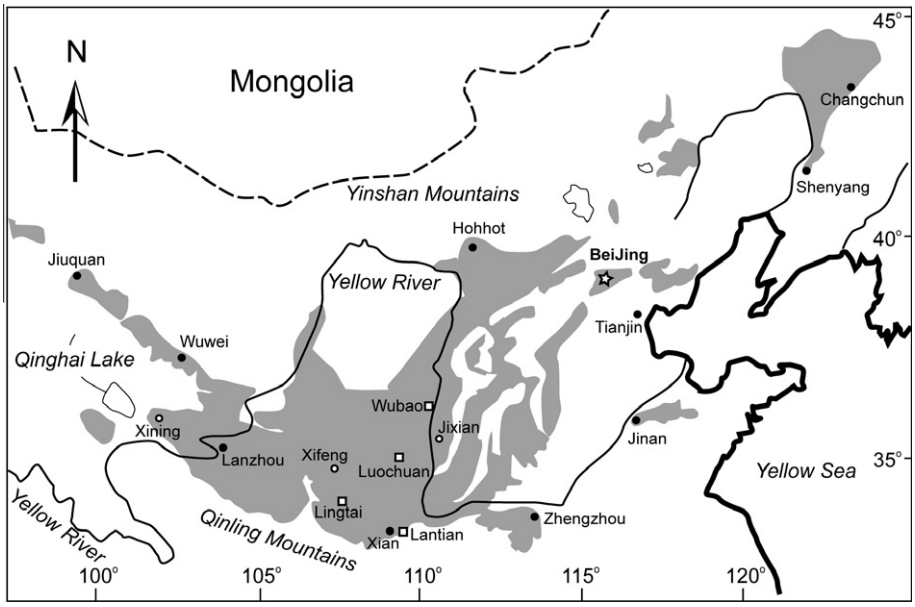

Fig. 1. Schematic map of the Chinese Loess Plateau showing the sampling sites of Lingtai, Wubao, Lantian and Luochuan (open squares). Modified from Jahn et al. (2001). Open circles represent the sample locations of Xining, Xifeng, Jixian in Peucker-Ehrenbrink and Jahn (2001).

Table 1
Sampling localities.

Sample No.	Location	Longitude, latitude	Sampling depth	Description
L1-WB-006-1,2,3	Wubao Xingzita section in Shaanxi province	110°42′E, 37°30′N	2–7 m	Malan loess
LT-DJ-L1-5	Lantian Duanjiapo section in Shaanxi province	109°12′E, 34°12′N	2–7 m	Malan loess
LT-DJ-L2-14	Lantian Duanjiapo section in Shaanxi province	109°12′E, 34°12′N	9.5–13.5 m	2nd layer of loess
L1-LUO-1	Luochuan Heimugou section in Shaanxi province	109°25′E, 35°45′N	1–9 m	Malan loess
L1-LUO-4	Luochuan Heimugou section in Shaanxi province	109°25′E, 35°45′N	1–9 m	Malan loess
LT-E3	Lingtai Renjiapo section in Gansu province	107°24′E, 35°02′N	255 m	Red clay
LT-L33	Lingtai Renjiapo section in Gansu province	107°24′E, 35°02′N	130 m	33rd layer of loess

Table 2
Major element concentrations of basaltic reference materials (wt.%).

	BCR-2 ($n = 4$)			GSR-3 ($n = 4$)		
	Mean	RSD%	Reference	Mean	RSD%	Reference
SiO_2	54.0	0.2	54.1	44.7	0.1	44.6
TiO_2	2.24	1.0	2.26	2.37	0.5	2.37
Al_2O_3	13.4	0.2	13.5	13.8	0.2	13.8
TFe_2O_3	13.8	0.2	13.8	13.4	0.4	13.4
MnO	0.188	2.7	0.19	0.162	3.9	0.17
MgO	3.69	1.5	3.59	7.75	0.4	7.77
CaO	7.13	0.2	7.12	8.84	0.2	8.81
Na_2O	3.22	1.3	3.16	3.40	0.9	3.38
K_2O	1.81	0.6	1.79	2.32	0.3	2.32
P_2O_5	0.348	1.4	0.35	0.943	0.5	0.95

BCR-2 and GSR-3 are USGS and Chinese reference materials, respectively. Reference values are from http://minerals.cr.usgs.gov/geo_chem_stand/ and Govindaraju (1994).

final solution was allowed to cool, stored overnight, and centrifuged shortly before measurement by ICP-MS.

An Agilent 7700x quadrupole ICP-MS at the Australian National University (ANU), was used to measure the isotopes of PGE and Re, except for sample L1-Wb-006–1,2,3 for which an Agilent 7500 quadrupole ICP-MS was used. The sensitivities for the Agilent 7700x were 2.1×10^5 cps (counts per second)/ppb (ng/g) for mass 89, 2.3×10^5 cps/ppb for mass 140 and 1.5×10^5 cps/ppb for mass 205. The sensitivities for the Agilent 7500 were about a factor of 10

Table 3
Trace element concentrations of the four rock reference materials analyzed in this study (ppm).

	BCR-2 ($n = 4$), Basalt			BHVO-2 ($n = 5$), Basalt			AGV-2 ($n = 5$), Andesite			SCo-1 ($n = 2$), Shale		
	Mean	RSD%	Reference	Mean	RSD%	Reference	Mean	RSD%	Reference	Mean	RSD%	Reference
Li	8.48	0.8	9	4.36	5.4	4.8	10.25	3.9	11	46.7	0.7	45
Be	1.94	4.1		0.98	6.7	1	2.09	4.8	2.3	1.81	6.1	1.84
Sc	32.9	2.7	33	31.6	0.9	32	12.9	1.9	13	11.8	2.0	10.8
V	413	2.0	416	324	0.5	317	120	2.8	122	130	3.2	131
Cr	15.2	4.8	18	285	1.2	280	15.6	6.4	16	68.9	0.7	68
Co	37.5	2.7	37	45.8	0.8	45	15.8	2.0	16	11.0	4.1	10.5
Ni	12.4	4.5	18	122	1.2	119	18.8	1.5	20	26.6	4.8	27
Cu	18.8	3.3	21	133	3.2	127	52.0	2.8	53	28.1	5.6	28.7
Zn	127	1.9	127	101	0.5	103	87.0	1.9	86	98.1	2.9	103
Ga	21.7	2.2	23	21.4	1.6	22	20.4	1.1	20	16.4	3.6	15
Ge	1.53	1.2		1.60	6.1	1.6	1.15	7.7		1.63	4.1	1
Rb	46.4	4.1	46.9	9.02	3.5	9.11	66.8	4.0	66.3	112	0.7	112
Sr	339	1.4	340	397	0.9	396	659	1.3	661	167	0.5	174
Y	36.8	2.1	37	26.1	1.7	26	19.5	2.4	19	24.9	1.2	26
Zr	182	1.6	184	169	1.0	172	229	1.1	230	167	2.7	160
Nb	12.3	2.9	12.6	18.6	1.9	18.1	14.1	2.7	14.5	11.9	0.7	11
Mo	248	1.6	250	3.91	6.7	4	2.01	6.0		1.21	0.9	1.37
Cd	0.15	14		0.07	12	0.06	0.063	8.4		0.13	22	0.14
Sn	2.17	2.1		1.89	6.8	1.7	2.17	6.2	2.3	3.31	4.7	3.7
Cs	1.14	2.5	1.1	0.10	4.9	0.1	1.14	2.6	1.2	7.87	2.7	7.8
Ba	677	1.6	677	128	4.8	131	1123	0.7	1130	585	0.5	570
La	25.0	3.8	24.9	15.2	3.3	15.2	38.8	3.0	37.9	29.2	2.8	29.5
Ce	53.2	0.9	52.9	37.4	1.8	37.5	70.1	3.0	68.6	58.1	2.8	62
Pr	6.76	2.1	6.7	5.27	1.9	5.35	8.05	1.4	7.84	6.85	0.5	6.6
Nd	29.1	1.8	28.7	24.7	2.1	24.5	30.7	1.5	30.5	26.5	1.9	26
Sm	6.71	1.7	6.58	6.13	2.6	6.07	5.56	2.2	5.49	5.16	0.6	5.3
Eu	1.98	1.5	1.96	2.03	1.6	2.07	1.60	2.6	1.53	1.14	1.2	1.19
Gd	6.80	1.6	6.75	6.22	2.2	6.24	4.71	2.0	4.52	4.51	0.1	4.6
Tb	1.09	1.9	1.07	0.95	2.2	0.92	0.66	1.4	0.64	0.72	3.0	0.7
Dy	6.49	1.9	6.41	5.37	2.5	5.31	3.56	2.5	3.47	4.15	0.2	4.2
Ho	1.30	1.9	1.28	0.97	2.6	0.98	0.66	2.7	0.65	0.85	2.1	0.97
Er	3.65	3.0	3.66	2.51	2.8	2.54	1.84	3.3	1.81	2.41	3.3	2.5
Tm	0.53	1.3	0.54	0.33	3.7	0.33	0.26	2.3	0.26	0.38	6.0	0.42
Yb	3.38	2.2	3.38	1.96	2.8	2	1.63	3.2	1.62	2.41	5.3	2.27
Lu	0.51	1.7	0.503	0.27	4.8	0.274	0.25	3.7	0.247	0.37	4.2	0.34
Hf	4.98	2.9	4.9	4.36	2.9	4.36	5.17	1.7	5	4.51	1.7	4.6
Ta	0.79	2.4	0.74	1.18	2.5	1.14	0.84	3.5	0.87	0.88	0.0	0.92
W	0.59	8.3		0.28	13	0.21	0.56	11		1.58	3.4	1.4
Tl	0.26	5.1		0.025	5.6	0.028	0.27	2.9	0.27	0.72	4.9	0.72
Pb	10.8	3.0	11	1.71	6.2	1.6	13.0	3.3	13.2	30.1	2.2	31
Bi	0.063	12		0.016	17		0.055	12		0.42	9.9	0.37
Th	5.90	3.5	5.7	1.20	2.4	1.22	6.13	1.1	6.1	9.58	0.2	9.7
U	1.66	1.5	1.69	0.41	3.3	0.403	1.86	2.0	1.86	3.07	0.3	3

The RSD is the relative standard deviation in percent. The reference values of BCR-2, BHVO-2 and AGV-2 are taken from the preferred values in the GeoReM database (http://georem.mpch-mainz.gwdg.de/). The reference values of SCo-1 are taken from Govindaraju (1994).

lower (2.0–2.7 $\times$ 10^4 cps/ppb for mass 89, 140 and 205). Solutions of Ni, Cu, Zn, Co, Hf, Mo, Zr and Ta were analyzed to monitor molecular isobaric interferences. These are potential matrix elements that may be present in sufficient concentrations in the dissolved Ni–sulfide beads to affect the measured PGE abundances. Argide production rates range from 0.002% to 0.008% for the Agilent 7700x, whereas they are about 2–5 times higher (0.005–0.016%) for the Agilent 7500. The effects of the molecular interference on all PGE were negligible (<0.3%), except for Ru. The Ni argide ($^{61,62}Ni^{40}Ar$) interference on Ru was subtracted using the measured argide production rates and the ^{61}Ni count rate. The corrections are generally less than 25% except for two analyses of sample L1-luo-4 (67%) and L1-Wb-006 (530%). Concentrations of Pd, Pt, Ir, Ru and Re were determined by isotope dilution using the $^{105}Pd/^{108}Pd$, $^{195}Pt/^{194}Pt$, $^{191}Ir/^{193}Ir$, $^{99}Ru/^{101}Ru$ and $^{185}Re/^{187}Re$ ratios, respectively. Ru concentrations are also calculated using $^{99}Ru/^{102}Ru$ and the results, with the exception of sample L1-Wb-006 (Table 4), agreed to within 10% of Ru concentrations calculated from $^{99}Ru/^{101}Ru$. Concentrations of the monoisotopic Rh were obtained using the method described in Meisel et al. (2003). This uses the count rates of ^{103}Rh and ^{106}Pd, with the assumption that

Table 4
Concentrations of platinum group elements and Re in Chinese loess and TDB-1 (ppb).

Sample	Ir	Ru	Rh	Pt	Pd	Re	Ru_N/Ir_N
L1-WB-006-1,2,3[a]	0.020	*0.020 (0.013)*	0.017	0.421	0.379	0.473	0.67
LT-DJ-L1-5	0.024	0.036 (0.034)	0.022	0.628	0.677	0.067	0.96
LT-DJ-L2-14	0.021	0.030 (0.029)	0.019	1.410	0.546	0.122	0.92
L1-luo-1	0.021	0.028 (0.024)	0.017	0.789	0.570	0.274	0.84
L1-luo-4	0.014	*0.017 (0.016)*	0.013	0.603	0.457	0.116	0.81
LT-E3	0.035	0.045 (0.041)	0.023	4.205[b]	0.668	0.077	0.82
LT-L33	0.024	0.036 (0.034)	0.019	0.658	0.521	0.101	0.95
Average	0.023	0.030	0.018	0.751	0.546	0.176	0.85
Median	0.021	0.030	0.019	0.643	0.546	0.116	
TDB-1							
This study ($n = 6$)	0.058 ± 0.006	0.152 ± 0.023	0.367 ± 0.061	4.16 ± 0.57	22.0 ± 5.0	0.67 ± 0.10	
M&M[c] ($n = 7$)	0.075 ± 0.018	0.198 ± 0.016	0.471 ± 0.078	5.01 ± 0.34	24.3 ± 3.4	0.79 ± 0.04	
P[d] ($n = 8$)	0.078 ± 0.006			4.40 ± 0.30	24.8 ± 1.4		
Certified[e]	0.15	0.30	0.70	5.80	22.4		

Samples with Ni-interference correction >25% are presented in *italics*.
Numbers in brakets are Ru concentrations calculated using $^{99}Ru/^{102}Ru$.
Uncertainties are quoted at the 2σ level.
[a] Analyzed using Agilent 7500 ICP-MS. Other samples are analyzed using Agilent 7700x ICP-MS.
[b] Excluded from average and median calculation.
[c] Meisel and Moser (2004), high pressure asher digestion and isotope dilution-ICP-MS.
[d] Peucker-Ehrenbrink et al. (2003), Ni–sulfide fire assay and isotope dilution-ICP-MS.
[e] Govindaraju (1994), Note that Ir, Ru and Rh values are provisional.

any loss of Rh during the analytical procedure was similar to loss of Pd. The detailed calculation procedure is described in Appendix A.

Procedural blanks were determined from sample-free analyses using 10 g of sodium borax, 1 g of Ni and 0.5 g of S for every session. Average procedural blanks based on three separate fusion blanks were 0.8 ± 0.2 ppt for Ir, 1.6 ± 0.9 ppt for Ru, 0.6 ± 0.1 ppt for Rh, 6.4 ± 1.1 ppt for Pt, 18.8 ± 1.9 ppt for Pd and 16.1 ± 0.7 ppt for Re. All data for the samples reported in Table 4 are blank corrected. The method detection limits (MDL), taken to be three standard deviations of the procedural blanks, were 0.6 ppt for Ir, 2.7 ppt for Ru, 0.3 ppt for Rh, 3.2 ppt for Pt, 5.8 ppt for Pd and 2.1 ppt for Re. The combined uncertainties (1σ RSD) arising from ICP-MS counting statistics, the PGE calibration standard, and blank subtraction are better than 5% for all of the PGE data except Ru, where uncertainties can reach 12%. This relatively large uncertainty reflects the variability of Ni–argide interferences on Ru. Accuracy and precision of measurements were tested by replicate analyses of the reference material TDB-1 (CANMET diabase). This sample was chosen because it has the lowest PGE and Re abundances among all the available reference materials and it has a homogeneous PGE and Re distribution at a sample sizes as small as 2 g (Meisel and Moser, 2004). The TDB-1 analyses carried out for this study gave a reproducibility of RSD <12% for all the PGE and Re, and are also consistent with the values reported by Meisel and Moser (2004) and Peucker-Ehrenbrink et al. (2003) (Table 4).

3. RESULTS

Major and trace elements data are reported in Table 5. In Fig. 2, the results are normalized to the UCC (McLennan, 2001; Hu and Gao, 2008). Most elements show a typical UCC distribution though some display negative and/or positive anomalies. Strontium and Na, which are easily mobilized during continental weathering (Nesbitt and Young, 1982; Jahn et al., 2001), show negative anomalies. Calcium concentrations are variable, showing both positive and negative anomalies. The highly variable Ca is a common feature of loess worldwide with the variation being related to their carbonate content (Jahn et al., 2001). Cesium concentrations are slightly elevated due to the absorption of Cs onto clay minerals (Gallet et al., 1998; Jahn et al., 2001). Also shown in Fig. 2 for comparison is the composition of the Chinese loess samples analyzed for PGE and Re in the study of Peucker-Ehrenbrink and Jahn (2001) (data from Jahn et al. (2001)). The compositions of the Chinese loess analyzed for this study agree well with those reported in Jahn et al. (2001) sharing the same Sr, Na and Ca anomalies. This suggests that the loess samples used in both studies have the same provenance and underwent similar evolutionary histories following their deposition.

PGE and Re data are reported in Table 4. Fig. 3a shows primitive mantle-normalized PGE and Re patterns for the Chinese loess. Also shown in Fig. 3a for comparison is the previously reported Chinese loess PGE and Re data from Peucker-Ehrenbrink and Jahn (2001). The PGE and Re patterns are parallel to each other with the exception of two samples that show positive Pt and Re anomalies. Iridium, Pd and Re concentrations of Chinese loess were found to lie within the ranges of 0.014–0.035, 0.379–0.677 and 0.067–0.473 ppb, respectively. These ranges are consistent with those of previously reported data for Chinese loess by Peucker-Ehrenbrink and Jahn (2001) (Fig. 3a). Rhodium concentrations, reported here for the first time in loess, range from 0.013 to 0.023 ppb, with an average (arithmetic mean)

Table 5
Major (wt.%) and trace element (ppm) compositions of the Chinese loess.

Analysis No.	N101535	N101526	N101519	N101545	N101542	N101517	N101508
Sample name	L1-Wb-006-1.2.3	LT-DJ-L1-5	LT-DJ-L2-14	L1-Luo-1	L1-Luo-4	LT-E3	LT-L-33
Location	Wubao	Lantian	Lantian	Luochuan	Luochuan	Lingtai	Lingtai
Recalculated compositions on a volatile-free basis							
SiO_2	66.35	66.39	61.36	64.19	64.64	66.82	65.92
TiO_2	0.66	0.82	0.70	0.70	0.67	0.83	0.77
Al_2O_3	12.47	15.87	13.68	13.55	13.00	16.10	14.83
Fe_2O_3	4.59	6.33	5.29	5.14	4.84	6.51	5.81
MnO	0.09	0.11	0.10	0.10	0.09	0.12	0.11
MgO	2.74	2.33	2.34	2.54	2.42	2.81	2.34
CaO	8.35	3.77	12.13	8.86	9.52	2.25	5.66
Na_2O	2.09	1.61	1.62	1.98	2.03	1.20	1.47
K_2O	2.49	2.65	2.59	2.77	2.62	3.22	2.90
P_2O_5	0.15	0.12	0.18	0.17	0.17	0.14	0.18
Total	100	100	100	100	100	100	100
LOI	8.37	7.19	11.74	9.29	9.22	6.7	7.96
CIA	57	66	63	59	58	68	65
Li	38.4	62.1	35.4	33.9	33.9	47.8	42.6
Be	1.82	2.52	1.85	1.77	1.63	2.36	2.16
Sc	10.9	15.6	12.0	11.4	11.0	14.2	13.1
V	76.9	112	86.4	82.1	79.4	109	94.9
Cr	65.4	89.1	63.9	66.6	62.2	81.5	71.5
Co	11.6	17.4	13.4	12.4	12.1	16.2	14.9
Ni	31.0	46.8	35.6	33.2	31.6	47.2	41.6
Cu	21.5	31.6	25.7	24.4	23.4	37.3	30.8
Zn	58.7	79.8	66.0	63.1	59.3	88.2	76.4
Ga	13.9	20.2	15.2	14.6	14.2	18.5	17.1
Ge	1.47	1.75	1.43	1.45	1.45	1.53	1.52
Rb	90.4	124	100	99.0	94.3	126	114
Sr	302	146	192	205	221	141	151
Y	29.2	34.2	27.9	27.5	27.0	30.3	30.9
Zr	231	248	194	201	216	218	226
Nb	13.1	17.2	13.9	13.6	13.1	15.8	15.4
Mo	0.77	0.86	0.71	1.03	0.78	1.16	0.91
Cd	0.087	0.11	0.094	0.095	0.095	0.067	0.11
Sn	2.43	3.37	2.70	2.69	2.54	3.32	2.99
Cs	6.36	10.4	7.77	7.62	6.84	10.9	8.61
Ba	473	603	483	504	489	570	505
La	33.3	42.7	33.9	33.9	32.3	36.1	35.2
Ce	67.9	87.8	69.0	67.6	65.7	78.7	72.3
Pr	7.57	9.58	7.65	7.62	7.28	8.25	8.22
Nd	29.3	36.9	29.9	30.0	28.1	32.4	31.6
Sm	5.82	7.20	5.78	5.79	5.63	6.31	6.27
Eu	1.11	1.40	1.20	1.20	1.16	1.29	1.24
Gd	5.25	6.58	5.40	5.63	5.34	5.89	5.64
Tb	0.82	1.00	0.85	0.85	0.80	0.93	0.87
Dy	4.87	5.66	4.76	4.98	4.72	5.28	5.11
Ho	0.98	1.15	0.95	0.97	0.93	1.08	1.00
Er	2.85	3.26	2.78	2.82	2.71	3.11	2.91
Tm	0.43	0.48	0.42	0.41	0.37	0.48	0.43
Yb	2.77	3.12	2.61	2.68	2.58	2.99	2.80
Lu	0.42	0.47	0.41	0.40	0.40	0.47	0.42
Hf	6.07	6.34	5.32	5.86	5.90	6.24	5.92
Ta	0.95	1.21	1.06	1.06	0.94	1.20	1.04
W	1.78	2.44	1.91	1.91	1.79	2.32	2.04
Tl	0.53	0.72	0.56	0.58	0.52	0.74	0.62
Pb	17.4	25.0	20.5	20.6	18.9	28.0	21.8
Bi	0.34	0.49	0.40	0.39	0.33	0.54	0.45
Th	11.0	16.7	12.5	13.7	11.5	15.4	13.0
U	2.87	2.78	2.78	2.63	2.40	2.95	2.55

CIA (chemical index of alteration) values were calculated according to the method of McLennan (1993) in which the contribution of carbonate to the total CaO was taken into consideration.

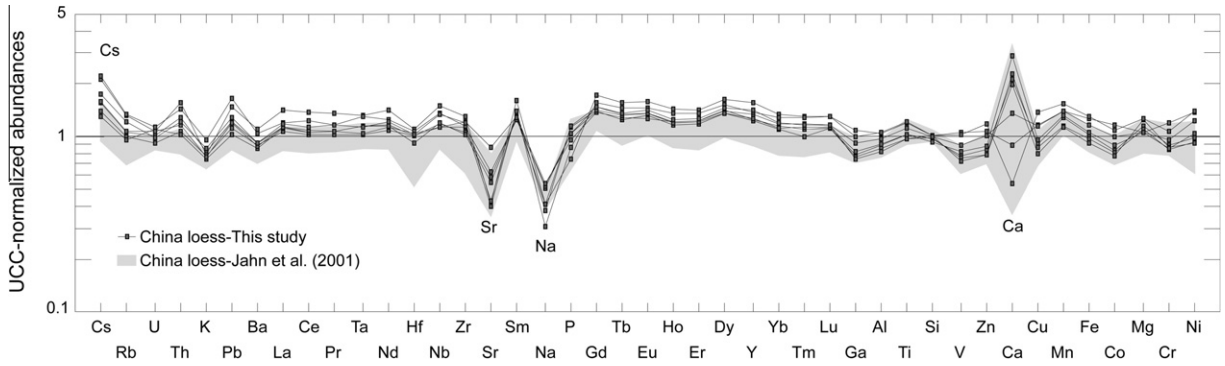

Fig. 2. UCC-normalized trace element diagrams for the Chinese loess analyzed in this study. Major and trace elements concentrations in Chinese loess analyzed for PGE and Re in Peucker-Ehrenbrink and Jahn (2001) (gray area; data from Jahn et al. (2001)) are also presented for comparison. The UCC values are from McLennan (2001) and Hu and Gao (2008). The element order follows Hofmann (1988), which is determined by the order of decreasing normalized concentrations of the UCC against the primitive mantle. Chinese loess shows typical UCC composition with exception of Cs, Sr, Na and Ca.

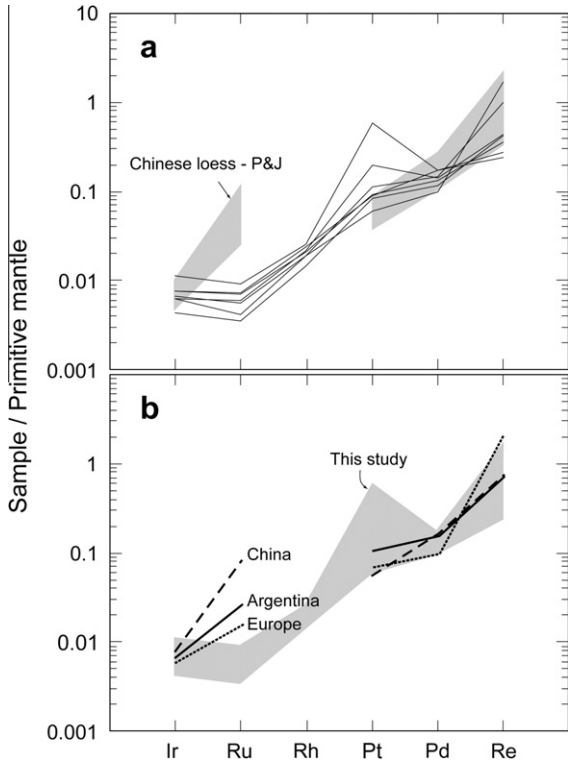

Fig. 3. (a) Primitive mantle normalized PGE and Re abundances in Chinese loess. Our results (solid lines) are compared with previous study (gray area; Peucker-Ehrenbrink and Jahn, 2001). (b) Average primitive mantle normalized PGE and Re concentrations in loess from China ($n = 6$), Argentina ($n = 3$) and Europe ($n = 7$) from previous study (Peucker-Ehrenbrink and Jahn, 2001). Our results (gray area) are shown for comparison. Primitive mantle values are from McDonough and Sun (1995).

and median values of 0.018 and 0.019 ppb respectively. The Pt concentrations range from 0.421 to 1.41 ppb and are comparable to those reported in Peucker-Ehrenbrink and Jahn (2001), except for one sample (LT-E3) that contains an abnormally high Pt content of 4.21 ppb. The most conspicuous feature of our data is that our Ru values are an order of magnitude lower than those reported by Peucker-Ehrenbrink and Jahn (2001) and show no hint of the positive Ru anomaly seen in the previous study (Fig. 3). Ruthenium concentrations in this study range from 0.017 to 0.045 ppb and have the same average and median value of 0.030 ppb (Table 4).

4. DISCUSSION

4.1. The Ru problem

Our PGE and Re data for Chinese loess agree with the values from Peucker-Ehrenbrink and Jahn (2001), except for Ru, for which our values are considerably lower (Fig. 3a). Since loess contains a wide variety of grains from different sources, heterogeneity is potentially a problem, and PGE and Re abundances can vary according to the predominant lithologies present in the contributing provenances (e.g. Peucker-Ehrenbrink and Jahn, 2001). For example, Argentine loess ($n = 3$) and European loess ($n = 7$) contain less PGE and Re than Chinese loess samples (Peucker-Ehrenbrink and Jahn, 2001). In the case of the Argentine loess, this may be attributed to a high volcaniclastic input and considerable riverine transport (Peucker-Ehrenbrink and Jahn, 2001).

Despite the potential for compositional variation, Chinese loess is reasonably homogeneous. Gallet et al. (1996) and Jahn et al. (2001) investigated the composition of Chinese loess from four different sections, which form a transect across the Chinese Loess Plateau from west to east (~800 km), and showed homogeneous major and trace elements and a restricted range of Sr–Nd isotopic compositions, indicating a provenance of relatively young and uniform upper crustal sources for the loess. The major and trace elements pattern of the Chinese loess reported in this study is almost identical to that reported in previous studies (Gallet et al., 1998; Jahn et al., 2001) (Fig. 2), including the samples used for PGE and Re analysis in the study of Peucker-Ehrenbrink and Jahn (2001), which confirms the geochemical homogeneity of the Chinese loess. The compiled PGE data (except Ru) for the Chinese loess reported in this study

($n = 7$), and those of Peucker-Ehrenbrink and Jahn (2001) ($n = 6$), show that the concentrations vary by only a factor of 3, which indicates homogeneous distribution of the PGE in the Chinese Loess Plateau. During loess formation Ru is likely to be hosted in sulfide, Cr spinel and alloy particulates along with other PGE (e.g. Cabri et al., 1996; Naldrett, 2004; Barnes et al., 2008; Brenan et al., 2012; Park et al., 2012). Therefore, if the observed difference in Ru was caused by source variation or transportation/deposition processes, it would have also influenced the other PGE to a similar extent. However, our Ir, Pt, Pd and Re data for the Chinese loess are remarkably similar to the values from Peucker-Ehrenbrink and Jahn (2001).

It should also be noted that the PGE patterns of Chinese loess reported in Peucker-Ehrenbrink and Jahn (2001) differ from those of various sedimentary and igneous rocks especially in terms of their very high Ru_N/Ir_N value (average 10.8, range: 3.6–15.9). Loess dusts originate from upper crustal rocks and include material from sedimentary, igneous rocks, and low-medium grade metamorphic rocks. Fig. 4 shows a compilation of PGE data for sedimentary and basaltic-andesitic intrusive and extrusive rocks from a wide range of localities, including flood basalts from the Tarim basin and gabbros from the Tahu basin in NW China, both of which are prospective source materials for the Chinese loess. Although the absolute concentrations vary by an order of magnitude, the PGE patterns of various types of sedimentary rocks are similar to each other. Notably, the Ru_N/Ir_N ratios show very limited variation, ranging from 1.1 to 1.8 (Fig. 4a). Importantly, this ratio does not vary between sedimentary and basaltic-andesitic igneous rocks, which also show similar PGE patterns with low Ru_N/Ir_N ratio of 0.5–1.5 (Fig. 4b). However, felsic igneous rocks dominate over basaltic rocks in the UCC (Wedepohl, 1995; Gao et al., 1998). Unfortunately, there are no data of Ru and Ir contents for felsic igneous rocks in the literature, but it is unlikely that the Ru_N/Ir_N of these rocks are higher than those of the mafic rocks since no fractional crystallization process that preferentially enriches Ru relative to the other PGE is known. Specifically, Ru and Ir have similar compatibility in potential host phases such as sulfide, Cr spinel and Os–Ir–Ru alloy (e.g. Cabri et al., 1996; Naldrett, 2004; Barnes et al., 2008; Brenan et al., 2012; Park et al., 2012) and thus magma differentiation cannot effectively fractionate Ru from Ir.

Based on the above discussion, we suggest the Ru data and high Ru_N/Ir_N values of Chinese loess samples shown in Peucker-Ehrenbrink and Jahn (2001) are an analytical artifact, rather than true geochemical characteristics of loess. Peucker-Ehrenbrink and Jahn (2001) used a Ni–sulfide fire assay – isotope dilution procedure (Ravizza and Pyle, 1997) for PGE analysis that is similar to the method employed here. Analyses of Ru with this method are often hindered by large molecular interferences from Ni-argide, requiring an additional process to separate Ni from a solution for ICP-MS (Ravizza and Pyle, 1997). This problem was circumvented here through use of the Agilent 7700x ICP-MS, which produced low Ni-argide production rates (0.003–0.004%), thus allowing for accurate correction of the NiAr interferences on Ru. Ruthenium concentrations calculated using $^{99}Ru/^{101}Ru$ and $^{99}Ru/^{102}Ru$ agree well (better than 10%; Table 4), except for one sample (L1-Wb-006-1,2,3) that was analyzed using an Agilent 7500 ICP-MS and has a major Ni-argide interference correction (530%). Despite this huge correction, the Ru data and primitive mantle normalized PGE pattern of L1-Wb-006-1,2,3

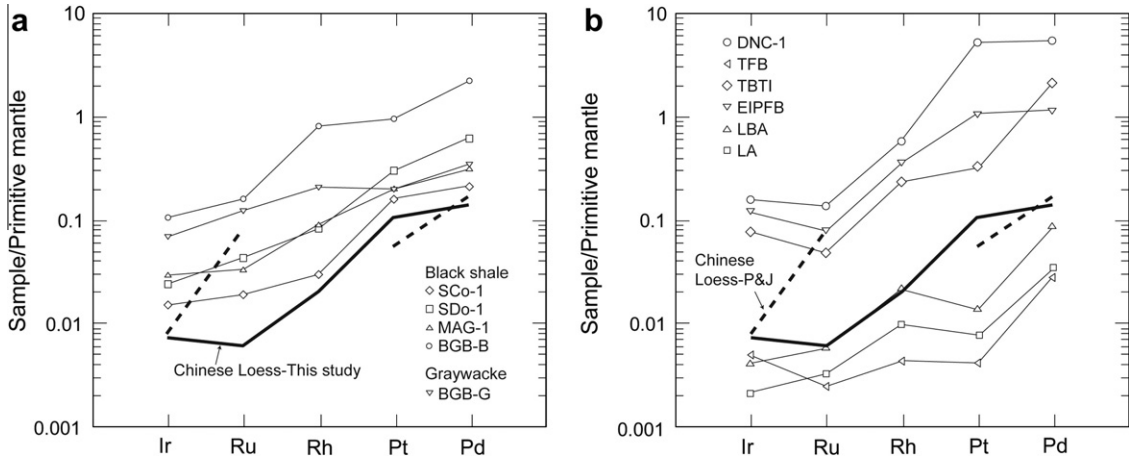

Fig. 4. (a) Compilation of PGE data from sedimentary rocks. Data sets from Meisel and Moser (2004): SCo-1 = Upper Cretaceous silty marine shale, Natrona Co., Wyoming; SDo-1 = Devonian Ohio Shale, USGS standard reference material; MAG-1 = recent marine mud, Gulf of Maine. Data sets from Siebert et al. (2005): BAB-B = Barberton Greenstone Belt Black shale, South Africa; BGB-G = Barberton Greenstone Belt Graywacke, South Africa. BAB-B ($n = 8$) and BGB-G ($n = 3$) are averaged values. (b) Compilation of PGE data from igneous rocks. DNC-1 = Triassic–Jurassic dolerite, North Carolina, USA (Meisel and Moser, 2004). TFB = Continental flood basalts ($n = 11$) from the Tarim basin, NW China (Yuan et al., 2012). TBTI = gabbro ($n = 1$) from the Tianyou intrusion, Tuha basin, NW China (Tang et al., 2011). EIPFB = Continental flood basalts ($n = 6$) from the Emeishian large igneous province, SW China (Zhang et al., 2005). LBA = basaltic andesites ($n = 3$), Leiqiong, SE China (Yang et al., 2011). LA = andesites ($n = 6$), Sanshui, SE China (Yang et al., 2011). Average PGE concentrations in Chinese loess from this study (solid line) and Peucker-Ehrenbrink and Jahn (2001) (dashed line) are shown for comparison. P&J represents Peucker-Ehrenbrink and Jahn (2001).

are consistent with those for other samples analyzed in this study, which suggests that the correction is reliable.

4.2. Platinum group elements in the upper continental crust

Peucker-Ehrenbrink and Jahn (2001) estimated the Ir and Pd concentrations in the UCC by averaging data for loess from China, Argentina and Europe and obtained values of 0.022 and 0.52 ppb, respectively. The compiled Ir and Pd data from this study and Peucker-Ehrenbrink and Jahn (2001) produce almost identical results (Ir = 0.022 ppb, Pd = 0.53 ppb). Inter-element correlations between Ni, Cr and Ir and Pd independently confirm that these values are good upper crustal estimates. The positive correlations of Ir with Ni ($r^2 = 0.50$) and Cr ($r^2 = 0.49$) yield Ir concentrations of 0.022 ppb and 0.021 ppb, respectively at upper crustal Ni and Cr concentrations (Ni = 34 ppm (μg/g), Cr = 73 ppm; Hu and Gao, 2008) (Fig. 5a and b). The correlations between Pd and Ni ($r^2 = 0.40$), and Pd and Cr ($r^2 = 0.59$) yield Pd concentrations of 0.56 and 0.58 ppb, respectively at upper crustal Ni and Cr concentrations (Fig. 5c and d). Compiled estimates of PGE and Re concentrations in the UCC are presented in Table 6 and Fig. 6. The revised Ir data of 0.022 ppb agrees with other upper crustal

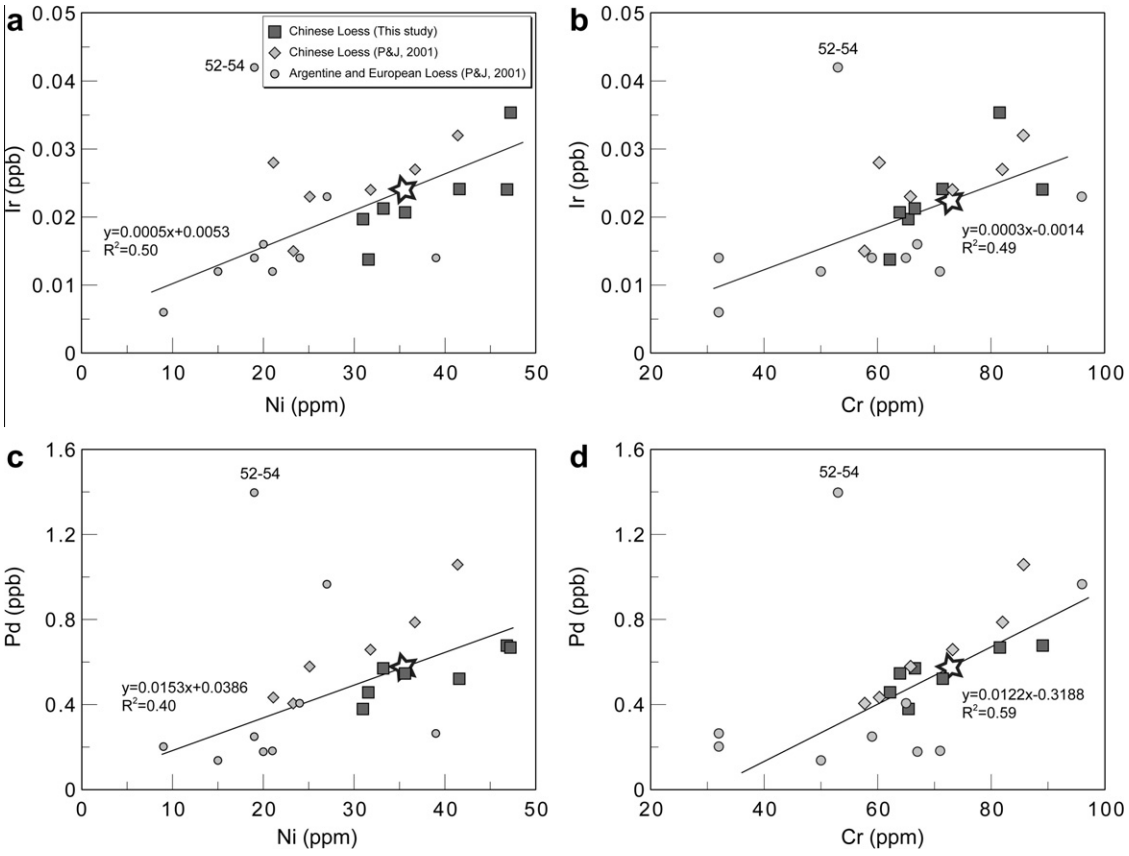

Fig. 5. Correlations between (a) Ir and Ni, (b) Ir and Cr, (c) Pd and Ni and (d) Pd and Cr in loess from China, Argentina and Europe from Peucker-Ehrenbrink and Jahn (2001) and this study. Sample 52–54 is excluded for linear regression. Average upper crustal compositions are shown as stars.

Table 6
Selected estimates of PGE and Re concentrations in the upper continental crust (ppb).

References	Ir	Ru	Rh	Pt	Pd	Re
Taylor and McLennan (1985, 1995)	0.020				0.500	0.400[a]
Wedepohl (1995)	0.050	0.100	0.060	0.400	0.400	0.400[a]
Schmidt et al. (1997)	0.03 ± 0.02[b]	1.06 ± 0.23	0.38 ± 0.21	1.50 ± 0.50	2.00 ± 0.52	0.40 ± 0.20
Gao et al. (1998)				1.500	1.460	
Peucker-Ehrenbrink and Jahn (2001)	0.022	0.210		0.510	0.520	0.198
This study	0.022	0.030	0.018	0.599	0.526	0.198[c]

[a] Esser and Turekian (1993).
[b] Derived from the data in Schmidt and Pernicka (1994).
[c] Peucker-Ehrenbrink and Jahn (2001).

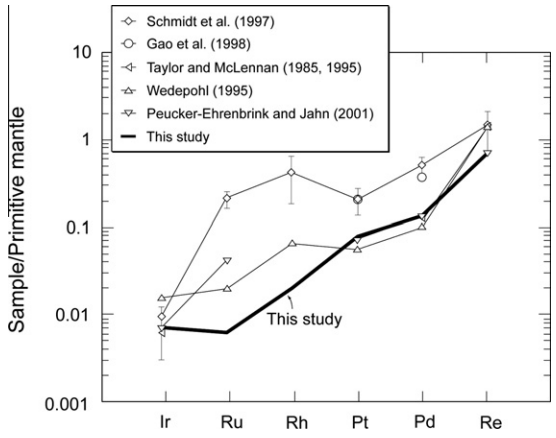

Fig. 6. Concentrations of platinum group elements and Re in the upper continental crust. Our estimates for the UCC, after omitting one sample with an anomalously high Pt content, are shown as a thick solid line. See text for discussion. Primitive mantle values are from McDonough and Sun (1995).

estimates within a factor of 2. The Pd data (0.53 ppb) is comparable to some estimates (0.5 ppb, Taylor and McLennan, 1985; 0.4 ppb, Wedepohl, 1995), but is nearly three times lower than those of Gao et al. (1998) and Schmidt et al. (1997).

The weighted average of Pt in loess from China, Argentina and Europe using the compiled Pt data from this study and Peucker-Ehrenbrink and Jahn (2001) is 0.73 ppb, which is ~ 50% higher than the previous estimate of 0.51 ppb of Peucker-Ehrenbrink and Jahn (2001) if one sample from this study, with an anomalously high Pt content (LT-E3, 4.21 ppb), is included. It should be noted that the Pt concentrations of loess are more variable than those of the other PGE (This study; Peucker-Ehrenbrink and Jahn, 2001). Furthermore, Pt variations are not correlated with the other PGE, which show strong correlations each other (Fig. 7). This decoupling suggests that Pt input during loess formation is controlled by at least two phases; one that contains all PGE in similar proportions, whereas the other is primarily enriched in Pt, suggesting a Pt–alloy. Magmatic Pt-alloys have been found as dominant host phases of Pt in some arc basalts and picrites from Ambae, Vanuatu (Park et al., 2012) and in chromitites and dunites from the Alaskan-type complexes, Urals (Garuti et al., 2003; Zaccarini et al., 2010). It is unlikely that the Pt variation is caused by alteration because Pt is not normally mobile during weathering (Jaffe et al., 2002). If we exclude sample LT-E3, which may be affected by the presence of Pt-enriched nugget effects, the weighted average Pt concentration of loess from China, Argentina and Europe is 0.60 ppb. Independent confirmation of this value as an estimate of the UCC, using inter-element correlations between Pt and other compatible elements such as Ni or Cr, was impossible due to the prohibitively weak correlations between Pt and these elements. Our value for Pt is comparable to the estimates of Wedepohl (1995) (0.4 ppb), but three times lower than that of Gao et al. (1998) (1.5 ppb) (Table 6 and Fig. 6).

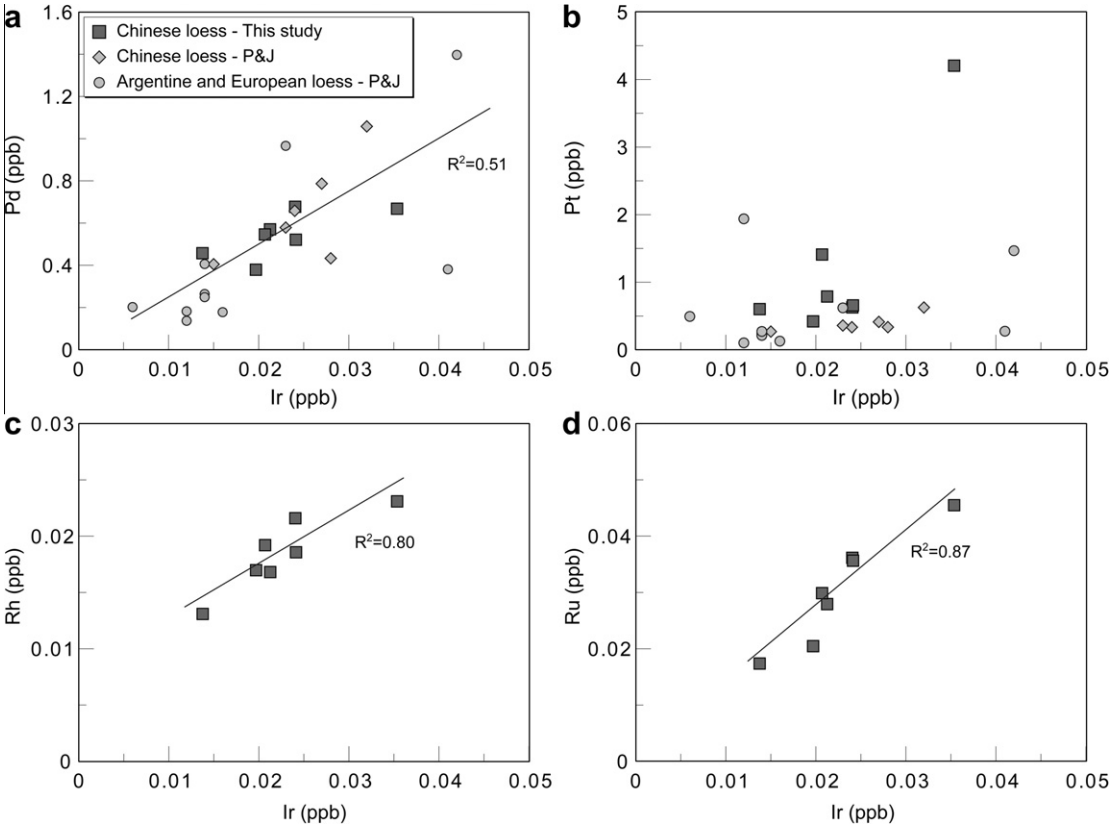

Fig. 7. (a–d) Pd, Pt, Rh and Ru variations against Ir in loess. P&J represents Peucker-Ehrenbrink and Jahn (2001).

The Ru data of Peucker-Ehrenbrink and Jahn (2001) are significantly higher than those obtained in this study, which results in Ru_N/Ir_N values that are 5–10 times higher (average 10.9, range: 3.6–15.9) than those of possible source rocks ($Ru_N/Ir_N = 0.5–1.8$) (Fig. 3). We have argued that the high Ru data come from unrecognized analytical artifacts. Due to the Ru problem, and the paucity of Rh data for loess in the literature, we only used our results for estimating the Ru and Rh concentrations in the UCC. The average concentrations are 0.030 ppb for Ru and 0.018 ppb for Rh. The Ru and Rh data show good correlations with Fe_2O_3 and transition metals such as Ni, Cr and Co ($r^2 = 0.56–0.89$) (Figs. 8 and 9). These correlations yield Ru and Rh concentrations of 0.026–0.036 and 0.016–0.022 ppb, respectively, at upper crustal Fe_2O_3, Ni, Cr and Co abundances ($Fe_2O_3 = 5.93$ wt.% (g/100 g), Ni = 34 ppm, Cr = 73 ppm and Co = 15 ppm; Hu and Gao, 2008), which agree well with our average Ru and Rh concentrations of 0.030 and 0.018 ppb, respectively. This provides independent confirmation that the average Ru and Rh concentrations in loess are good upper crustal estimates. Notably, these values are about 3 times lower than those of Wedepohl (1995) (Ru = 0.1 ppb, Rh = 0.06 ppb) and 10–15 times lower than those of Schmidt et al. (1997) (Ru = 1.06 ± 0.23 ppb, Rh = 0.38 ± 0.21 ppb).

As is evident from the above discussion, existing estimates of average PGE concentrations in the UCC are highly variable (Table 6 and Fig. 6). The most widely used estimates are those of Schmidt et al. (1997) and Wedepohl (1995). Schmidt et al. (1997) estimated PGE abundances in the UCC using the PGE concentrations of the impact melts from two Scandinavian craters (Mien and Dellen, Sweden), after they had been corrected for the PGE contents of the meteoric component. However, the sizes of the Mien and Dellen craters are too small (10–20 km in diameter) to provide a representative sample of the UCC, and this method has significant uncertainties originating from estimating the meteoritic contribution and correcting for it. Use of this method to estimate the UCC composition should be restricted to the impact

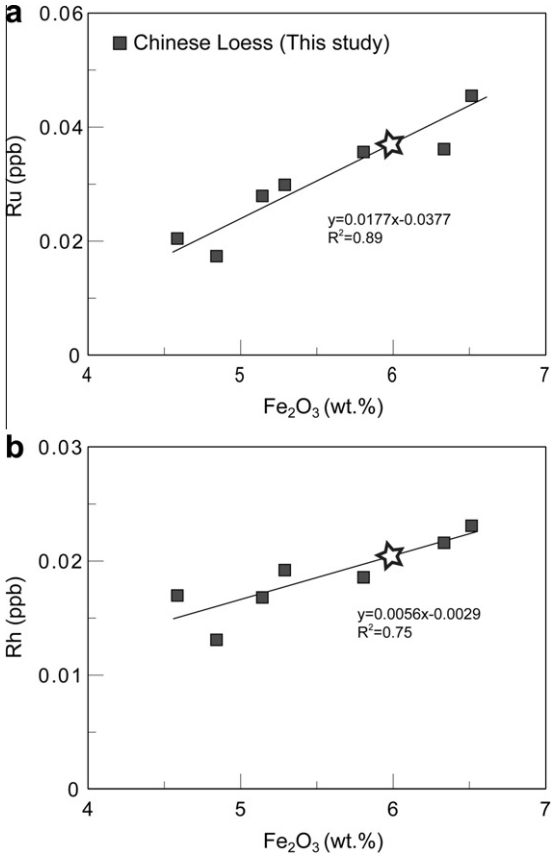

Fig. 8. Correlations between (a) Ru and Fe_2O_3 and (b) Rh and Fe_2O_3 in Chinese loess analyzed in this study. Average upper crustal compositions are shown as stars.

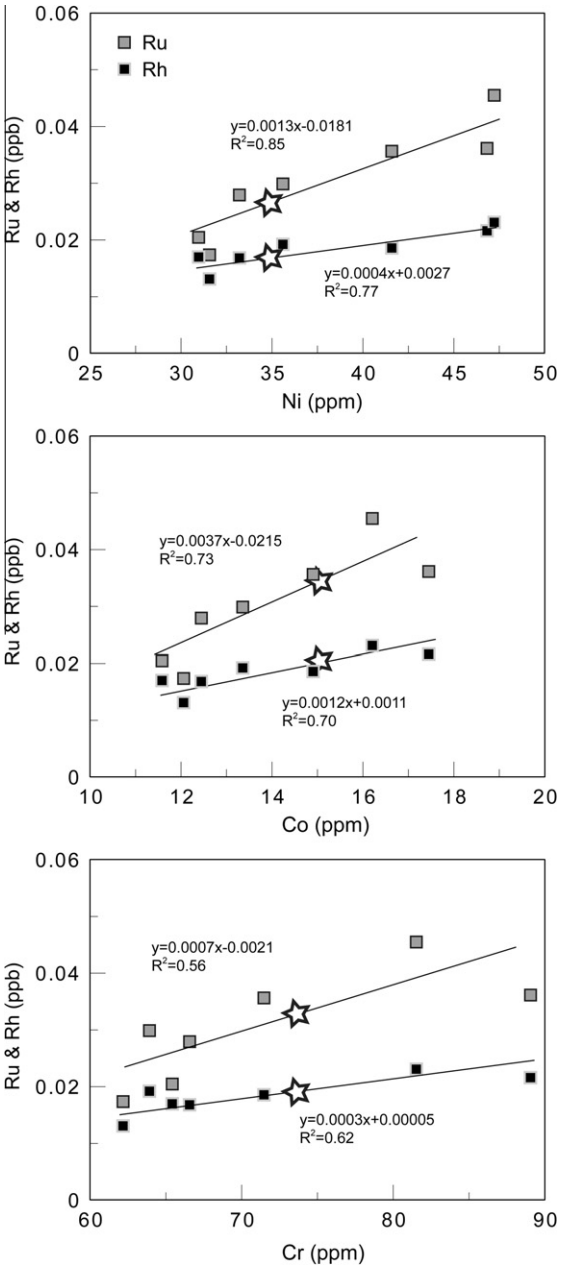

Fig. 9. Correlations between Ru, Rh and Ni, Co, Cr in Chinese loess analyzed in this study. Average upper crustal compositions are shown as stars.

melts from craters that are significantly larger (>50–100 km in diameter) in continental shield areas. The significantly elevated PGE estimates by Schmidt et al. (1997) may result from PGE-enriched local rocks in the Mien and Dellen areas or an underestimation of the meteoritic component.

Wedepohl (1995) reported average PGE contents for 17 European graywackes to estimate the PGE concentrations of the UCC. The PGE patterns in sediments can vary regionally according to the predominant lithologies, therefore graywackes from other continents should also be considered to estimate the UCC composition. Furthermore, in contrast to loess, the detritus in sedimentary rocks such as shales and greywackes are altered by weathering, transport and diagenesis, which can result in mobility and loss of some of the PGE (Peucker-Ehrenbrink and Hannigan, 2000; Jaffe et al., 2002).

Loess samples crustal rocks from large geographical areas and is only marginally affected by chemical weathering (Flint, 1947; Smalley, 1966, 1995; Smalley and Cabrera, 1970; Hu and Gao, 2008). However, eolian fractionation may affect the PGE budget of loess (Peucker-Ehrenbrink and Jahn, 2001) because PGE are likely to be hosted by heavy trace minerals such as sulfides and alloys. In fact, there are variations in grain size and composition from sand-rich loess (NNW) to clay-rich loess (SSE) in the central Chinese Loess Plateau (Eden et al., 1994). Also, loess is generally enriched in silica compared to other upper crustal rocks such as shale because of the mechanical and chemical durability of quartz during eolian transportation (e.g. Taylor et al., 1983; Hu and Gao, 2008). However, PGE concentrations of Chinese loess from seven different sections vary by only a factor of 3 (except for Pt in sample LT-E3) (Fig. 3a) and there is no significant correlation between PGE contents and the sample location, showing that the PGE were homogeneously distributed in the central Chinese Loess Plateau. Furthermore, the average Zr content of loess lies within the range of estimates for the UCC (Fig. 2; This study; Gallet et al., 1998; Jahn et al., 2001) despite the fact that Zr is concentrated in zircon, a heavy mineral. Here it should be remembered that size, not density, is the main factor controlling the transport of minerals by wind and water, and such that small zircon grains are the hydraulic equivalent of larger quartz grains. This supports our hypothesis that eolian transport and deposition processes did not significantly dilute or concentrate heavy phases, and consequently had no significant effect on PGE concentrations. We therefore propose that our new compilation of PGE data for loess from China, Argentina and Europe of Ir = 0.022 ppb, Ru = 0.030 ppb, Rh = 0.018 ppb, Pt = 0.60 ppb, and Pd = 0.53 ppb, provides the best available estimate for the PGE concentrations of the UCC.

4.3. Rhenium in the upper continental crust

Degradation of organic matter in sedimentary rocks results in a pronounced decrease in Re concentrations during the early stages of chemical weathering (Peucker-Ehrenbrink and Hannigan, 2000; Jaffe et al., 2002). Schnetger (1992) reported that loess generally contains low organic carbon contents (~0.1 wt.%). Although loess is influenced by limited chemical weathering, it appears that loess loses some Re during its formation (Peucker-Ehrenbrink and Jahn, 2001). The higher Re abundances observed for two samples (Fig. 3a) may be attributed to elevated organic carbon contents in these samples. Organic carbon data are therefore required to reconstruct initial Re concentrations in loess using the organic carbon/Re relationships for sedimentary rocks (Peucker-Ehrenbrink and Hannigan, 2000; Jaffe et al., 2002). Alternatively, Peucker-Ehrenbrink and Jahn (2001) adopted the approach of Esser and Turekian (1993) for calculating Re abundances using $^{187}Re/^{188}Os$ and Os concentrations and suggested that the average Re concentration of the UCC is 0.198 ppb.

The lack of organic carbon, Re-Os isotopic and concentration data for the Chinese loess analyzed in this study made it impossible to recalculate the initial Re concentrations prior to weathering. However, the Re data reported in this study have average and median values of 0.176 and 0.116 ppb, respectively, which are in general accord with the results of the previous study (0.206 and 0.126 ppb; Peucker-Ehrenbrink and Jahn, 2001). Thus, given the restricted range of $^{187}Re/^{188}Os$ ratios and Os concentrations previously observed for Chinese loess (Peucker-Ehrenbrink and Jahn, 2001), the reconstructed Re concentrations in our samples are likely to be similar to the value of 0.198 ppb reported by Peucker-Ehrenbrink and Jahn (2001).

5. CONCLUSIONS

The major and lithophile trace element concentrations of Chinese loess analyzed in this study show a typical upper crustal composition. The PGE abundances in these samples vary within a factor of 2 (except for Pt) and show similar primitive mantle normalized PGE patterns regardless of sampling location. The strong correlations ($R^2 = 0.40$–0.89) between the PGE (except for Pt) and other compatible elements, and subtle differences in the abundances of the PGE in Chinese loess from different provinces, suggest that eolian fractionation was not a significant influence on the distribution of the 'heavy' phases that carried the PGE. Our results show that the use of loess, which is the least affected by chemical weathering amongst sediments and samples rocks from a huge area, is the best way to constrain the PGE abundances of the UCC. We therefore propose revised estimates for the UCC abundances of Ir (0.022 ppb), Ru (0.030 ppb), Rh (0.018 ppb), Pt (0.60 ppb) and Pd (0.53 ppb) using a compilation of PGE data for loess from China, Argentina and Europe. Inter-element correlations between PGE and Fe_2O_3, Ni, Cr and Co observed in global loess independently confirm that these values are good upper crustal estimates.

ACKNOWLEDGEMENTS

This research was funded by an ARC Discovery Grant to Ian Campbell, the National Nature Science Foundation of China (41073020, 41173016, 91014007), the Fundamental Research Funds for the Central Universities and Chinese Ministry of Education (B07039). We thank Charlotte Allen for assistance with the ICP-

MS analysis and valuable comments. We also thank Paolo Sossi for help in English and constructive comments. This paper benefited greatly from reviews by Thomas Meisel and Bernhard Peucker-Ehrenbrink. We also thank Mark Rehkämper for the editorial handling.

APPENDIX A. PGE AND RE ANALYSIS PROCEDURE

PGE and Re concentrations were measured using a Ni–sulfide fire assay – isotope dilution method, which was described by Park et al. (2012). Ten grams of powdered sample were mixed with Ni, S and sodium borate powder (S252-10, Fisher Scientific) in the ratio of sample: Ni:S:Na-borax = 10:1:0.5:10, each weighed to 5 decimal places. These were mixed thoroughly on clean paper and transferred into porcelain Coors^{TM} crucibles. A mixed spike solution of PGE (^{99}Ru, ^{105}Pd, ^{185}Re, ^{191}Ir, and ^{195}Pt) was added into the sample powder and weighed. A second outside crucible, containing ~ 0.1 g of flour was used to provide reduced condition at the beginning of the fusion. The crucibles were dried in the furnace for 60 min at 100 °C to remove absorbed water from the sample. The mixture was then fused in a preheated furnace at 1100 °C for 40 min and quenched by removing the crucible from the furnace. N_2 gas was introduced into the open furnace with the flow rate of ~0.03 m^3/min to provide reducing conditions during fusion. After quenching, the crucible was broken open, and the Ni–sulfide beads were collected and dissolved in 150 ml of 6 mol/l HCl. The solutions were then filtered through a Millipore filter paper (0.45 μm cellulose membrane) and washed with Milli-Q water, prior to digestion in 4 ml aqua regia (1 ml of 14 mol/l HNO_3 and 3 ml of 8 mol/l HCl). All reagents used in this method were purified by a sub-boiling system (Savillex^{TM} DST-1000). After complete digestion, the solutions were dried down to approximately ~100 μl, then diluted with 5 ml of 2% HNO_3 and refluxed at 100 °C for 2 h. This final solution was allowed to cool, stored overnight, and centrifuged shortly before measurement by ICP-MS.

Concentrations of monoisotopic Rh were corrected by the method of Meisel et al. (2003), using count rates of ^{103}Rh and ^{106}Pd, making the assumption that any loss of Rh during the analytical procedure was similar to loss of Pd. The numbers of atoms of ^{103}Rh in the sample + spike mixture N_{mix}^{103Rh} is calculated as follows:

$$N_{mix}^{103Rh} = \frac{N_{mix}^{106Pd} \times C_{mix}^{103Rh}}{C_{mix}^{106Pd}} \times \frac{C_{standard}^{103Rh}}{C_{standard}^{106Pd}} \times \frac{N_{standard}^{103Rh}}{N_{standard}^{106Pd}}$$

where N_{mix}^{A} and $N_{standard}^{A}$ are the numbers of atoms of the isotope A in the sample + spike mixture and standard, respectively. C_{mix}^{A} and $C_{standard}^{A}$ are the count rates of the isotope A in the sample + spike mixture and standard, respectively.

REFERENCES

An Z. S., Kukla G. J., Porter S. C. and Xiao J. L. (1991) Magnetic susceptibility evidence of monsoon variation on the Loess Plateau of Central China during the last 130,000 years. *Quatern. Res.* **36**, 29–36.

Barnes S. J., Prichard H. M., Cox R. A., Fisher P. C. and Godel B. (2008) The location of the chalcophile and siderophile elements in platinum-group element ore deposits (a textural, microbeam and whole rock geochemical study): implications for the fortnation of the deposits. *Chem. Geol.* **248**, 295–317.

Barth M. G., McDonough W. F. and Rudnick R. L. (2000) Tracking the budget of Nb and Ta in the continental crust. *Chem. Geol.* **165**, 197–213.

Brenan J. M., Finnigan C. F., McDonough W. F. and Homolova V. (2012) Experimental constraints on the partitioning of Ru, Rh, Ir, Pt and Pd between chromite and silicate melt: the importance of ferric iron. *Chem. Geol.* **302**, 16–32.

Cabri L. J., Harris D. C. and Weiser T. W. (1996) Mineralogy and distribution of platinum-group mineral (PGM) placer deposits of the world. *Explor. Min. Geol.* **5**, 73–167.

Eden D. N., Wen Q. Z., Hunt J. L. and Whitton J. S. (1994) Mineralogical and geochemical trends across the Loess Plateau, North China. *Catena* **21**, 73–90.

Esser B. K. and Turekian K. K. (1993) The osmium isotopic composition of the continental-crust. *Geochim. Cosmochim. Acta* **57**, 3093–3104.

Flint R. F. (1947) *Glacial Geology and the Pleistocene Epoch*. John Wiley and Sons, Inc., New York.

Fritsche J. and Meisel T. (2004) Determination of anthropogenic input of Ru, Rh, Pd, Re, Os, Ir and Pt in soils along Austrian motorways by isotope ICP-MS. *Sci. Total Environ.* **325**, 145–154.

Gallet S., Jahn B. M. and Torii M. (1996) Geochemical characterization of the Luochuan loess-paleosol sequence, China, and paleoclimatic implications. *Chem. Geol.* **133**, 67–88.

Gallet S., Jahn B. M., Lanoe B. V., Dia A. and Rossello E. (1998) Loess geochemistry and its implications for particle origin and composition of the upper continental crust. *Earth Planet. Sci. Lett.* **156**, 157–172.

Gao S., Luo T. C., Zhang B. R., Zhang H. F., Han Y. W., Zhao Z. D. and Hu Y. K. (1998) Chemical composition of the continental crust as revealed by studies in East China. *Geochim. Cosmochim. Acta* **62**, 1959–1975.

Garuti G., Pushkarev E. V., Zaccarini F., Cabella R. and Anikina E. (2003) Chromite composition and platinum-group mineral assemblage in the Uktus Uralian-Alaskan-type complex (Central Urals, Russia). *Miner. Deposita* **38**, 312–326.

Govindaraju K. (1994) Compilation of working values and sample description for 383 geostandards. *Geostand. Newsl.* **18**, 1–158.

Guan Q. Y., Pan B. T., Gao H. S., Li N., Zhang H. and Wang J. P. (2008) Geochemical evidence of the Chinese loess provenance during the Late Pleistocene. *Palaeogeogr. Palaeoclimatol. Palaeoecol.* **270**, 53–58.

Guillong M., Danyushevsky L., Walle M. and Raveggi M. (2011) The effect of quadrupole ICPMS interface and ion lens design on argide formation. Implications for LA-ICPMS analysis of PGE's in geological samples. *J. Anal. At. Spectrom.* **26**, 1401–1407.

Hofmann A. W. (1988) Chemical differentiation of the earth - the relationship between mantle, continental-crust, and oceanic-crust. *Earth Planet. Sci. Lett.* **90**, 297–314.

Hooda P. S., Miller A. and Edwards A. C. (2008) The plant availability of auto-cast platinum group elements. *Environ. Geochem. Health* **30**, 135–139.

Hu Z. C. and Gao S. (2008) Upper crustal abundances of trace elements: a revision and update. *Chem. Geol.* **253**, 205–221.

Jaffe L. A., Peucker-Ehrenbrink B. and Petsch S. T. (2002) Mobility of rhenium, platinum group elements and organic carbon during black shale weathering. *Earth Planet. Sci. Lett.* **198**, 339–353.

Jahn B. M., Gallet S. and Han J. M. (2001) Geochemistry of the Xining, Xifeng and Jixian sections, Loess Plateau of China: eolian dust provenance and paleosol evolution during the last 140 ka. *Chem. Geol.* **178**, 71–94.

McDonough W. F. and Sun S. S. (1995) The composition of the earth. *Chem. Geol.* **120**, 223–253.

McLennan S. M. (1993) Weathering and global denudation. *J. Geol.* **101**, 295–303.

McLennan S. M. (2001) Relationships between the trace element composition of sedimentary rocks and upper continental crust. *Geochem. Geophys. Geosys.* **2**, 2000GC000109.

Meisel T. and Moser J. (2004) Platinum-group element and rhenium concentrations in low abundance reference materials. *Geostand. Geoanal. Res.* **28**, 233–250.

Meisel T., Fellner N. and Moser J. (2003) A simple procedure for the determination of platinum group elements and rhenium (Ru, Rh, Pd, Re, Os Ir and Pt) using ID-ICP-MS with an inexpensive on-line matrix separation in geological and environmental materials. *J. Anal. At. Spectrom.* **18**, 720–726.

Naldrett A. J. (2004) M*agmatic Sulfide Deposits. Geology, Geochemistry and Exploration*. Spiringer, Berlin.

Nesbitt H. W. and Young G. M. (1982) Early proterozoic climates and plate motions inferred from major element chemistry of lutites. *Nature* **299**, 715–717.

Pan S. H., Zhang G., Sun Y. L. and Chakraborty P. (2009) Accumulating characteristics of platinum group elements (PGE) in urban environments, China. *Sci. Total Environ.* **407**, 4248–4252.

Paquay F. S., Goderis S., Ravizza G., Vanhaecke F., Boyd M., Surovell T. A., Holliday V. T., Haynes C. V. and Claeys P. (2009) Absence of geochemical evidence for an impact event at the Bolling-Allerod/Younger Dryas transition. *Proc. Natl. Acad. Sci. U S A* **106**, 21505–21510.

Park J.-W., Campbell I. H. and Eggins S. M. (2012) Enrichment of Rh, Ru, Ir and Os in Cr spinels from oxidized magmas: evidence from the Ambae volcano, Vanuatu. *Geochim. Cosmochim. Acta* **78**, 28–50.

Peucker-Ehrenbrink B. and Hannigan R. E. (2000) Effects of black shale weathering on the mobility of rhenium and platinum group elements. *Geology* **28**, 475–478.

Peucker-Ehrenbrink B. and Jahn B. M. (2001) Rhenium-osmium isotope systematics and platinum group element concentrations: Loess and the upper continental crust. *Geochem. Geophys. Geosys.* 2, 2001GC000172.

Peucker-Ehrenbrink B., Bach W., Hart S. R., Blusztajn J. S. and Abbruzzese T. (2003) Rhenium-osmium isotope systematics and platinum group element concentrations in oceanic crust from DSDP/ODP Sites 504 and 417/418. Geochem. Geophys. Geosys. **4**, 2002GC000414.

Ravizza G. and Pyle D. (1997) PGE and Os isotopic analyses of single sample aliquots with NiS fire assay preconcentration. *Chem. Geol.* **141**, 251–268.

Schmidt G. and Pernicka E. (1994) The determination of Platinum-Group Elements (PGE) in target rocks and fall-back material of the nordlinger ries impact crater, Germany. *Geochim. Cosmochim. Acta* **58**, 5083–5090.

Schmidt G., Palme H. and Kratz K. L. (1997) Highly siderophile elements (Re, Os, Ir, Ru, Rh, Pd, An) in impact melts from three European impact craters (Saaksjarvi, Mien, and Dellen): clues to the nature of the impacting bodies. *Geochim. Cosmochim. Acta* **61**, 2977–2987.

Schnetger B. (1992) Chemical-composition of loess from a local and worldwide view. *Neus Jb. Miner. Monat.* **1**, 29–47.

Siebert C., Kramers J. D., Meisel T., Morel P. and Nagler T. F. (2005) PGE, Re-Os, and Mo isotope systematics in Archean and early Proterozoic sedimentary systems as proxies for redox conditions of the early Earth. *Geochim. Cosmochim. Acta* **69**, 1787–1801.

Smalley I. J. (1966) Properties of glacial loess and formation of loess deposits. *J. Sediment. Petrol.* **36**, 669–676.

Smalley I. (1995) Making the material: the formation of silt-sized primary mineral particles for loess deposits. *Quatern. Sci. Rev.* **14**, 645–651.

Smalley I. J. and Cabrera J. G. (1970) Shape and surface texture of loess particles. *Geol. Soc. Am. Bull.* **81**, 1591–1596.

Sun D. H., Liu T. S., Chen M. Y. and An Z. S. (1997) Magnetostratigraphy and palaeoclimate of Red Clay sequences from Chinese loess Plateau. *Sci. China Ser. D* **40**, 337–343.

Sun D. H., John S., An Z. S., Cheng M. Y. and Yue L. P. (1998) Magnetostratigraphy and paleoclimatic interpretation of a continuous 7.2 Ma Late Cenozoic eolian sediments from the Chinese Loess Plateau. *Geophys. Res. Lett.* **25**, 85–88.

Tagle R. and Berlin J. (2008) A database of chondrite analyses including platinum group elements, Ni, Co., Au, and Cr: implications for the identification of chondritic projectiles. *Meteorit. Planet. Sci.* **43**, 541–559.

Tagle R., Erzinger J., Hecht L., Schmitt R. T., Stoffler D. and Claeys P. (2004) Platinum group elements in impactites of the ICDP Chicxulub drill core Yaxcopoil-1: are there traces of the projectile? *Meteorit. Planet. Sci.* **39**, 1009–1016.

Tang D. M., Qin K. Z., Li C. S., Qi L., Su B. X. and Qu W. J. (2011) Zircon dating, Hf–Sr–Nd–Os isotopes and PGE geochemistry of the Tianyu sulfide-bearing mafic-ultramafic intrusion in the Central Asian Orogenic Belt, NW China. *Lithos* **126**, 84–98.

Taylor S. R. and McLennan S. M. (1985) *The continental crust: its composition and evolution*. Blackwell Scientific Publications, Oxford.

Taylor S. R. and McLennan S. M. (1995) The geochemical evolution of the continental crust. *Rev. Geophys.* **33**, 241–265.

Taylor S. R., Mclennan S. M. and Mcculloch M. T. (1983) Geochemistry of loess, continental crustal composition and crustal model ages. *Geochim. Cosmochim. Acta* **47**, 1897–1905.

Wang J. P. (2006) Formation and evolution of the middle reaches of the Yellow River since late Cenozoic. Ph. D thesis, Lanzhou University, 69–73 (in Chinese).

Wang X. S. and Sun C. (2009) Pt and Pd concentrations and source in urban roadside soils from Xuzhou. *China Environ. Geol.* **56**, 1129–1133.

Wedepohl K. H. (1995) The composition of the continental-crust. *Geochim. Cosmochim. Acta* **59**, 1217–1232.

Yang A. Y., Zhao T. P., Qi L., Yang S. H. and Zhou M. F. (2011) Chalcophile elemental constraints on sulfide-saturated fractionation of Cenozoic basalts and andesites in SE China. *Lithos* **127**, 323–335.

Yuan F., Zhou T., Zhang D., Jowitt S. M., Keays R. R., Liu S. and Fan Y. (2012) Siderophile and chalcophile metal variations in basalts: implications for the sulfide saturation history and Ni–Cu–PGE mineralization potential of the Tarim continental flood basalt province, Xinjiang Province, China. *Ore Geol. Rev.* **45**, 5–15.

Zaccarini F., Garuti G. and Pushkarev E. V. (2010) Unusual PGE-rich chromitite in the "Butyrin-Veins" of the Kytlym Ural-Alaskan complex (Northern Urals) 11th International Platinum Symposium, Sudbury, Ontario, Canada.

Zhang Z. C., Mao J. W., Mahoney J. J., Wang F. S. and Qu W. J. (2005) Platinum group elements in the Emeishan large igneous province, SW China: implications for mantle sources. *Geochem. J.* **39**, 371–382.

Associate editor: Mark Rehkamper